ARCH. MECH. TECH. MATER. VOL. 39, (2019) 66-73

DE GRUYTER OPEN

ARCHIVES OF MECHANICAL TECHNOLOGY AND MATERIALS
WWW.AMTM.PUT.POZNAN.PL

Geometrical structure of surface after turning of 316L stainless steel in laser assisted conditions

Michał Szymański[a], Mateusz Kukliński[a]

[a] *Poznań University of Technology, Faculty of Mechanical Engineering and Management, Institute of Mechanical Technology, Piotrowo 3, 60-965 Poznań, Poland*

[*] *Corresponding author, Tel.: +48-61 665-27-52, e-mail address: michal.mari.szymanski@doctorate.put.poznan.pl*

A R T I C L E I N F O

Received 18 June 2019
Received in revised form 25 November 2019
Accepted 31 December 2019

K E Y W O R D S

Surface roughness measurement
316L stainless steel
Turning
LAM

A B S T R A C T

The effects of turning 316L steel in a laser assisted machining are presented in this paper. The properties of 316L stainless steel are also shown in this article. In order to show correlation between the technological parameters, microgeometry of cutting tools and geometrical structure of surface, turning of material in grade 316L supported by laser has been executed. In addition, optical examination of cutting inserts has been performed and geometrical measurements of machined surfaces have been taken. The results of researches on the effects of the technological parameters and cutting tool's microgeometry on the geometrical structure of the 316L steel surface after turning in LAM conditions are described.

1. INTRODUCTION

Austenitic, corrosion-resistant stainless steels are a relatively large group of materials [2]. An example of this steel is 316L. The crystallographic structure of 316L steel consists of 53% of the cellular δ-ferrite, 45% of austenite and 2% of skeletal δ-ferrite [3]. The most important elements in this kind of steel are: chromium (16,5 – 18,5%), nickel (10 – 13 %) and molybdenum (2 – 2,5 %) [4]. 316L steel is a material used for making structural materials by SLM method [8]. It is also used as a porous implant material [5]. This type of steel is an example of a nonhardenable material. However, it is possible to treat this steel with cold work and annealing [1]. It is also characterized by a high thermal stability, which allows to use it in high temperature conditions [9]. The properties of 316L enable to use it in lots of applications, but on the other hand they cause difficulties in machining processes. Therefore, 316L stainless steel is an example of a difficult-to-machining material [1,4].

It is reasonable to perform 316L machining processes in LAM conditions, because they give satisfying technological and economical effects similar to machining materials like Inconel 718, Inconel 625 or stainless steel. A laser-assisted machining is a method of treatment in which the machined material is locally heated by a laser beam. The softened material is removed by a cutting tool. LAM processes make a treatment easier and contribute to the growth of machining efficiency and durability of cutting tools [6, 7, 11].

The aim of this research was to prove correlation between the cutting tool's microgeometry, technological parameters and the geometrical structure of the 316L steel surface after turning in LAM conditions. In this research two types of cutting inserts were used: SECO CNMG 120408-MF1 TM4000 and SAND CNMG 120408-MF 1115.

2. TURNING OF 316L STEEL IN LAM CONDITIONS

The turning process of 316L steel in LAM conditions was carried out on a laboratory station with a CNC lathe DMG CTX 310 ECOLINE and with a robot KUKA KR 16-2 with a laser head TRUMPF TruDiode 3006. The sample was a shaft made of 316L steel. The diameter of the shaft was approximately

DOI: 10.2478/amtm-2019-0012

72mm. The sample, shown in Fig. 1 had sixteen separated measurement sections.

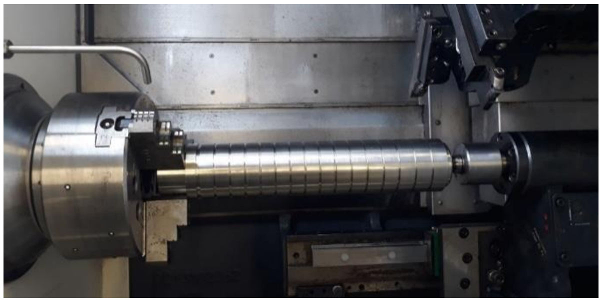

Fig. 1. The shaft made of 316L steel in the lathe spindle

During the turning process the shaft was lidded by Henkel Bonderite L-FG LS 2127 Acheson. This substance prevents reflection and scattering of the laser beam.

For each insert: SECO CNMG 120408-MF1 TM4000 and SAND CNMG 120408-MF 1115 8 series of tests were planned. The energy density of the laser beam *GE* =1,2J/mm², the diameter of the laser beam *dl* =1,2mm, the angle distance between the laser spot point and the tool's cutting edge ϕ= 45° were the constant technological parameters. The tests were carried out with variable technological parameters: cutting depth a_p=0,1mm,a_p=0,3mm, cutting speed v_c= 50m/min,v_c= 75m/min, feed rate*f*= 0,08mm/obr., *f*= 0,15mm/obr., power of laser beam *P*= 1200W, *P* = 1800W. The tests were carried out during longitudinal turning.

Cutting parameters used for tests are shown in Tab. 1.

Tab. 1. Cutting parameters used for tests

Type of inserts	Symbol	a_p	v_c	f
[-]	[-]	[mm]	[m/min]	[mm/rev]
SECO CNMG 120408-MF1 TM4000	C1	0,1	75	0,15
	C2	0,3	75	0,15
	C3	0,1	50	0,15
	C4	0,3	50	0,15
	C5	0,3	75	0,08
	C6	0,1	50	0,08
	C7	0,3	50	0,08
	C8	0,1	75	0,08
SAND CNMG 120408-MF 1115	S1	0,1	75	0,15
	S2	0,3	75	0,15
	S3	0,1	50	0,08
	S4	0,3	50	0,08
	S5	0,3	75	0,08
	S6	0,1	75	0,08
	S7	0,3	50	0,15
	S8	0,1	50	0,15

Fig. 2 shows the scheme of turning of 316L stainless steel in laser assisted conditions.

The measurements of surface roughness of the workpiece were carried out on a laboratory station with JENOPTIC HOMMEL – ETAMIC W5 and a computer. Five measurements of surface roughness were made for each measurement section. The measurements of surface roughness were carried out in conditions according to ISO 11562:1996. The measuring tip T1 was used. The values of λ_s and λ_f filters were not defined. The value of λ_c filter was 0,80mm. The value of l_p was 4,799mm. The values of l_r and l_w were 0,8mm. The value of mapping section was 4,80mm. The value of traverse speed was 0,50mm/s. The value of traverse length was 80µm. In these researchers the following parameters were tested: *Ra*, *Rz*, *Rt*.

The microscopic measurements of cutting tools were carried out on a ZEISS SteREO Discovery.V20.

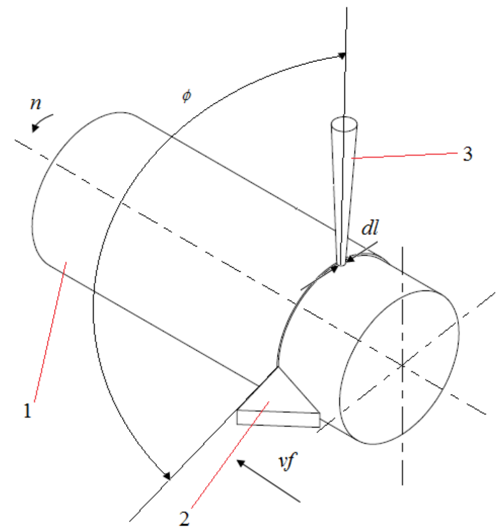

Fig. 2. The scheme of the turning process in LAM conditions: n –turning speed, v_f–feed speed, dl –diameter of the laser beam, ϕ – angle distance between the laser spot point and the tools' cutting edge, 1 – workpiece, 2 –cutting insert, 3 –laser beam

3. RESULTS AND DISCUSSION

Fig. 3 and Fig. 4 show results of the microscopic measurements of cutting inserts before turning (Fig. 3 a, c and Fig. 4 a, c) and after turning (Fig. 3 b, d and Fig. 4 b, d).

Fig. 3 shows that the technological parameters of turning in LAM conditions had a significant influence for cutting inserts condition. The built-up edge effect is noticeable on the A_γ surface. The cutting insert edge seems to be deformed between the A_γ surface and the A'_α surface. Effects of abrasive wear are not noticeable on the surface of cutting insert.

Fig. 4 shows that the technological parameters of turning in LAM conditions had a significant influence on cutting inserts condition. The built-up edge effect is noticeable on the A_γ surface, but it seems to be bigger than on the surfaces of the SECO CNMG 120408-MF1 TM4000 cutting insert. The main cutting edge is deformed between the A_γ surface and the A'_α surface. The effects of abrasive wear are not noticeable on the surface of cutting insert. The crack and the crater are visible on the A_γ surface. These effects are a sign that SAND CNMG 120408-MF cutting insert wore more than SECO CNMG 120408-MF1 TM4000 cutting insert. The cutting insert's coating was grinded.

Fig. 5 shows the evolution of *Ra* as a function of cutting depth a_p and cutting speed v_c after turning of 316L stainless steel in laser assisted conditions with SECO CNMG 120408-MF1 TM4000 cutting insert. It can be evidenced that the values of *Ra* decrease with the increase of the cutting speed v_c and with the increase of the cutting depth a_p. The highest value of *Ra* is obtained with the cutting speed v_c = 48m/min and with the cutting depth a_p = 0,08mm. The lowest value of

Ra is obtained with the cutting speed v_c = 76m/min and with the cutting depth a_p = 0,32mm.

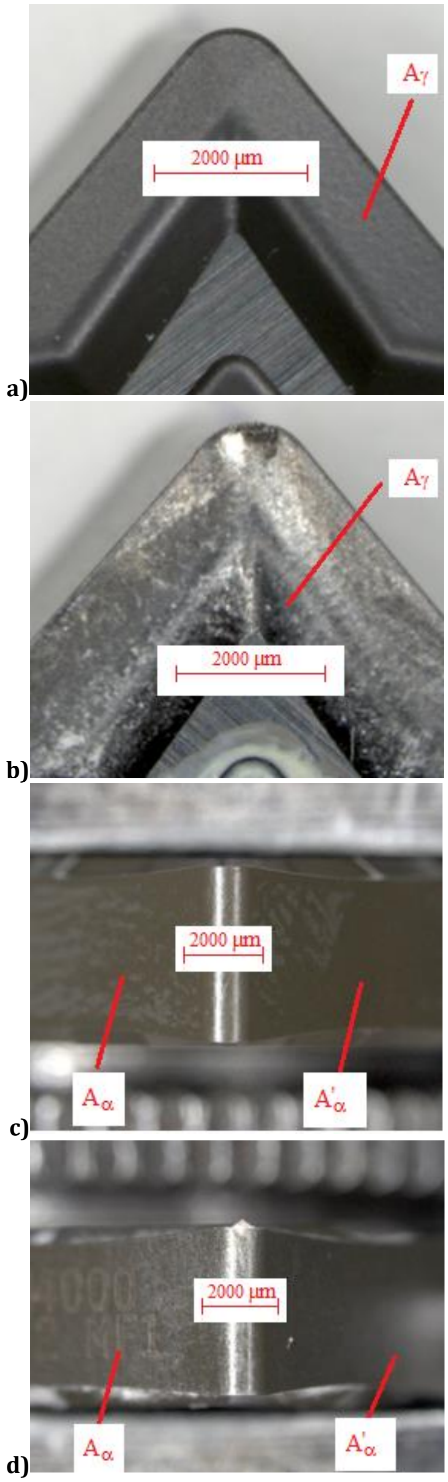

Fig. 3. Cutting insert SECO CNMG 120408-MF1 TM4000: a) and c) before turning, b) and d) after turning

Fig. 6 shows the evolution of *Ra* as a function of cutting depth a_p and feed rate *f* after turning of 316L stainless steel in laser assisted conditions with SECO CNMG 120408-MF1 TM4000 cutting insert. Fig. 6 shows that the values of *Ra* increase with the decrease of the cutting speed v_c and with the increase of the feed rate *f*. The highest value of *Ra* is obtained with the cutting speed v_c = 48m/min and with the feed rate *f* = 0,15/rev mm. The lowest value of *Ra* is obtained with the cutting speed v_c = 76m/min and with the feed rate *f* = 0,07mm/rev.

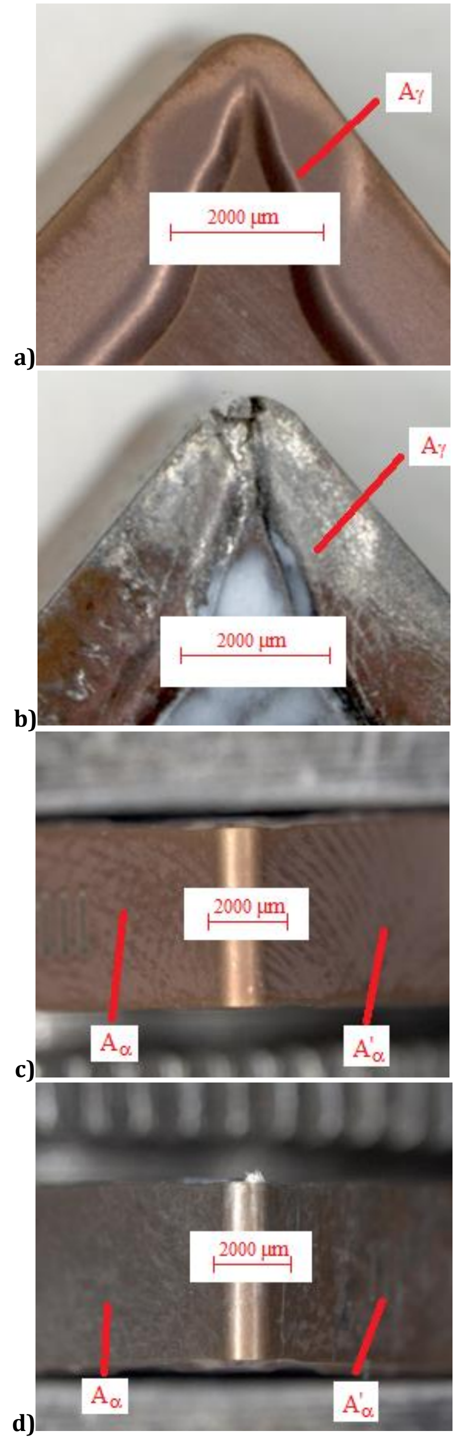

Fig. 4. Cutting insert SAND CNMG 120408-MF: a) and c) before turning, b) and d) after turning.

Fig. 7 shows the evolution of *Rz* as a function of cutting depth a_p and cutting speed v_c after turning of 316L stainless steel in laser assisted conditions with SECO CNMG 120408-

MF1 TM4000 cutting insert. After analyzing the graph, it can be stated that the values of *Rz* decrease with the increase of the cutting speed v_c and with the increase of the cutting depth a_p. The highest value of *Rz* is obtained with the cutting speed v_c = 48m/min and with the cutting depth a_p = 0,08mm. The lowest value of *Ra* is obtained with the cutting speed v_c = 76m/min and with the cutting depth a_p = 0,08mm. It does not confirm the correlation between the values of *Rz* and the values of the cutting depth a_p.

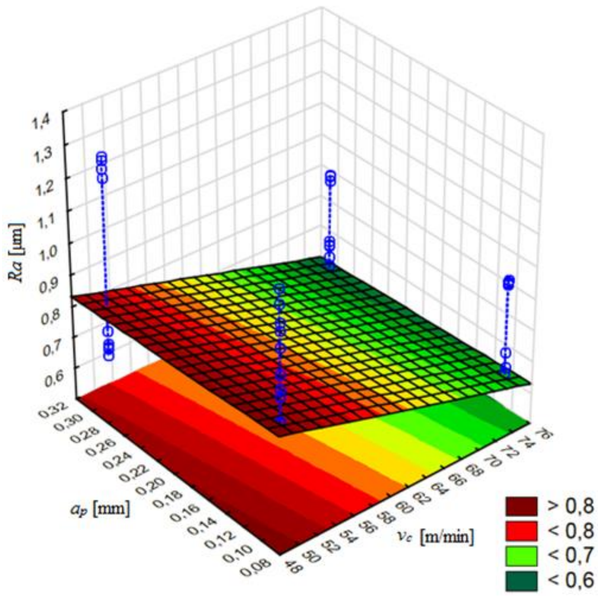

Fig. 5. Ra as a function of cutting speed v_c and cutting depth a_p after turning with SECO CNMG 120408-MF1 TM4000 cutting insert

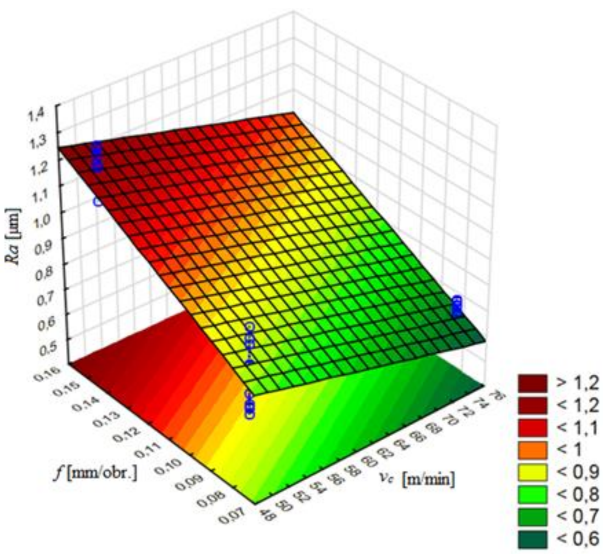

Fig. 6. Ra as a function of cutting speed v_c and feed rate f after turning with SECO CNMG 120408-MF1 TM4000 cutting insert

Fig. 8 shows the evolution of *Rz* as a function of cutting depth a_p and feed rate *f* after turning of 316L stainless steel in LAM conditions with SECO CNMG 120408-MF1 TM4000 cutting insert. It can be stated that the values of *Rz* increase with the decrease of the cutting speed v_c and with the increase of the feed rate *f*. The highest value of *Rz* is obtained with the cutting speed v_c = 48m/min and with the feed rate *f* = 0,16mm/rev. The lowest value of *Ra* is obtained with the cutting speed v_c = 76m/min and with the feed rate *f* = 0,16mm/rev. It does not confirm the correlation between the values of *Rz* and the values of the feed rate *f*.

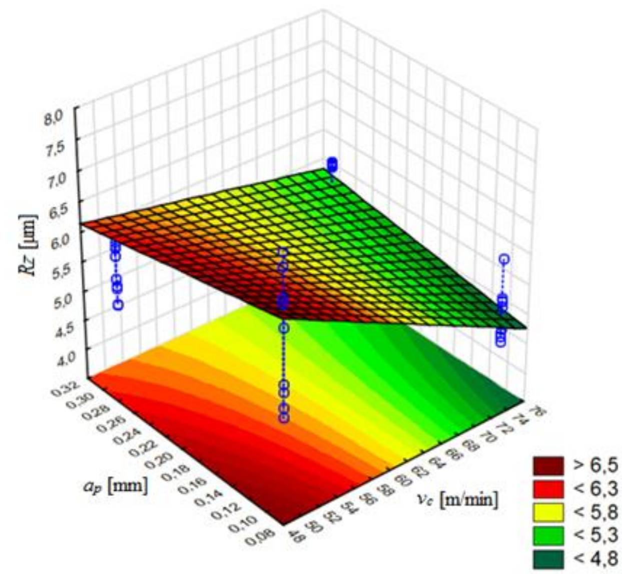

Fig. 7. Rz as a function of cutting speed v_c and cutting depth a_p after turning with SECO CNMG 120408-MF1 TM4000 cutting insert

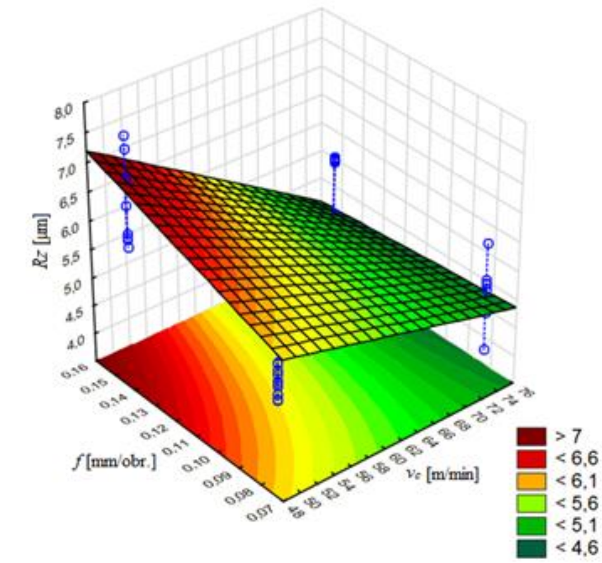

Fig. 8. Rz as a function of cutting speed v_c and feed rate f after turning with SECO CNMG 120408-MF1 TM4000 cutting insert

Fig. 9 shows the evolution of *Rt* as a function of cutting depth a_p and cutting speed v_c after turning of 316L stainless steel in laser assisted conditions with SECO CNMG 120408-MF1 TM4000 cutting insert. It can be evidenced that the values of *Rt* increase with the decrease of the cutting speed v_c and with the decrease of the cutting depth a_p. The highest value and the lowest value of *Rt* do not confirm correlation between the values of *Rt* and the values of the cutting depth a_p. The highest value of *Rt* is obtained with the cutting speed

v_c = 48m/min and with the cutting depth a_p = 0,08mm. The lowest value of *Rt* is obtained with the cutting speed v_c = 76m/min and with the cutting depth a_p = 0,08mm.

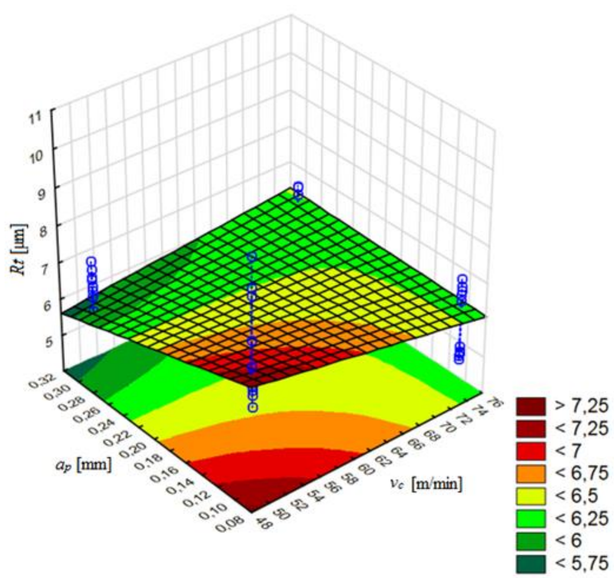

Fig. 9. Rt as a function of cutting speed v_c and cutting depth a_p after turning with SECO CNMG 120408-MF1 TM4000 cutting insert

Fig. 10 shows the evolution of *Rt* as a function of cutting depth a_p and feed rate *f* after turning of 316L stainless steel in laser assisted conditions with SECO CNMG 120408-MF1 TM4000 cutting insert. The highest value of *Rt* is obtained with the cutting speed v_c = 48m/min and with the feed rate *f* = 0,16mm/rev. The lowest value of *Rt* is obtained with the cutting speed v_c = 76m/min and with the feed rate *f* = 0,16mm/rev. It can be stated that the values of *Rt* increase with the decrease of the cutting speed v_c and with the increase of the feed rate *f*.

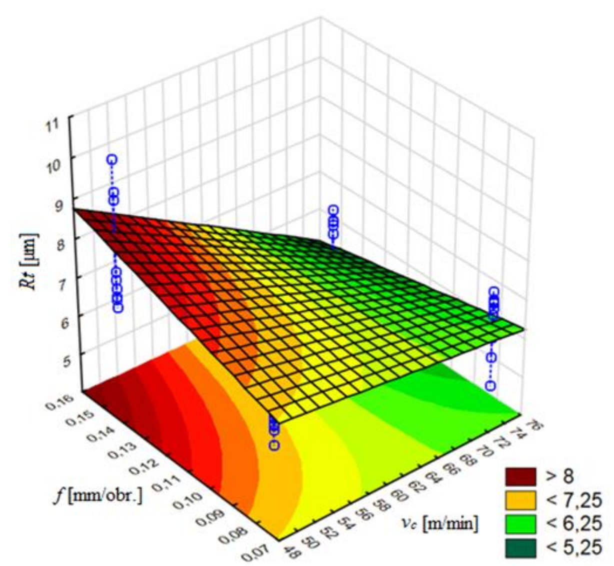

Fig. 10. Rt as a function of cutting speed v_c and feed rate f after turning with SECO CNMG 120408-MF1 TM4000 cutting insert

Fig. 11 shows the evolution of *Ra* as a function of cutting depth a_p and cutting speed v_c after turning of 316L stainless steel in laser assisted conditions with SAND CNMG 120408-MF cutting insert. After analyzing the graph, it can be stated that the highest value of *Ra* is obtained with the cutting speed v_c = 48m/min and with the cutting depth a_p = 0,32mm. The lowest value of *Ra* is obtained with the cutting speed v_c = 76m/min and with the cutting depth a_p = 0,08mm. It can be evidenced that the values of *Ra* increase with the decrease of the cutting speed v_c and with the increase of the cutting depth a_p.

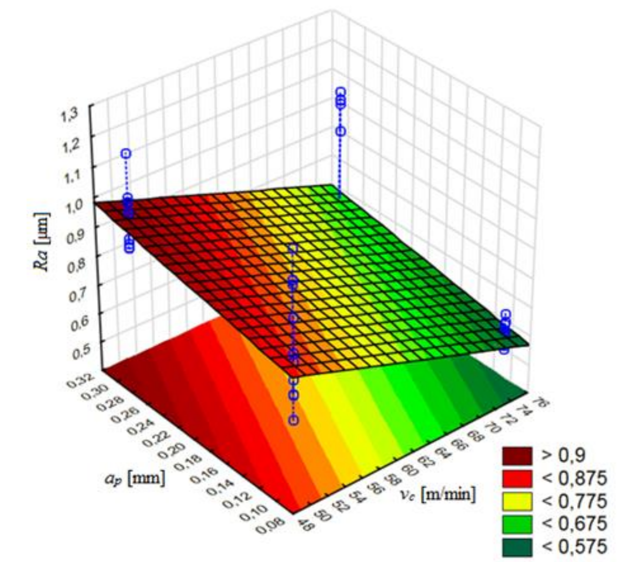

Fig. 11. Ra as a function of cutting speed v_c and cutting depth a_p after turning with SAND CNMG 120408-MF 1115 cutting insert

Fig. 12 shows the evolution of *Ra* as a function of cutting depth a_p and feed rate *f* after turning of 316L stainless steel in laser assisted conditions with SAND CNMG 120408-MF cutting insert. Fig. 12 shows that the values of *Ra* increase with the decrease of the cutting speed v_c. The values of *Ra* increase with the decrease of the feed rate *f*. The highest value of *Ra* is obtained with the cutting speed v_c = 48m/min and with the feed rate *f* = 0,07mm/rev. The lowest value of *Ra* is obtained with the cutting speed v_c = 76m/min and with the feed rate *f* = 0,16mm/rev.

Fig. 13 shows the evolution of *Rz* as a function of cutting depth a_p and cutting speed v_c after turning of 316L stainless steel in laser assisted conditions with SAND CNMG 120408-MF cutting insert. It can be evidenced that the values of *Rz* increase with the decrease of the cutting speed v_c and with the increase of the cutting depth a_p. After analyzing the graph, it can be stated that the highest value of *Ra* is obtained with the cutting speed v_c = 48m/min and with the cutting depth a_p = 0,32mm. The lowest value of *Ra* is obtained with the cutting speed v_c = 76m/min and with the cutting depth a_p = 0,08mm.

Fig. 14 shows the evolution of *Rz* as function of cutting depth a_p and feed rate *f* after turning of 316L stainless steel in laser assisted conditions with SAND CNMG 120408-MF cutting insert. It can be evidenced that the values of *Rz* increase with the decrease of the cutting speed v_c and with the decrease of the feed rate *f*. The highest value of *Rz* is obtained with the cutting speed v_c = 48m/min and with the feed rate *f* = 0,07mm/rev. The lowest value of *Rz* is obtained with the cutting speed v_c = 76m/min and with the feed rate f = 0,16mm/rev.

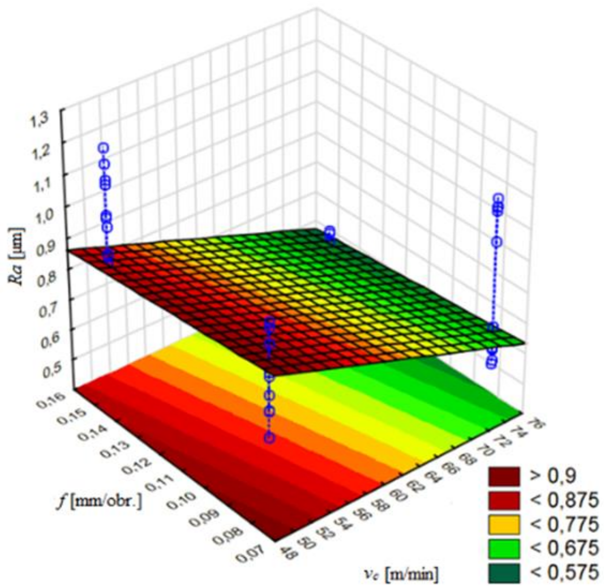

Fig. 12. Ra as a function of cutting speed v_c and feed rate f after turning with SAND CNMG 120408-MF 1115 cutting insert

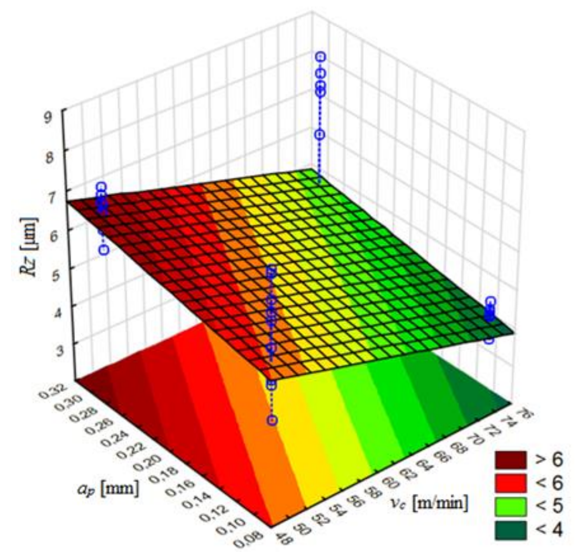

Fig. 13. Rz as a function of cutting speed v_c and cutting depth a_p after turning with SAND CNMG 120408-MF 1115 cutting insert

Fig. 15 shows the evolution of *Rt* as a function of cutting depth a_p and cutting speed v_c after turning of 316L stainless steel in laser assisted conditions with SAND CNMG 120408-MF cutting insert. After analyzing the graph, it can be stated that the highest value of *Rt* is obtained with the cutting speed v_c = 48m/min and with the cutting depth a_p = 0,32mm. The lowest value of *Rt* is obtained with the cutting speed v_c = 76m/min and with the cutting depth a_p = 0,08mm. It can be evidenced that the values of *Rt* increase with the decrease of the cutting speed v_c and with the increase of the cutting depth a_p. Correlations between the values of *Rt* and the values of the cutting speed v_c and the values of the cutting depth a_p were confirmed by the highest and the lowest values of *Rt*.

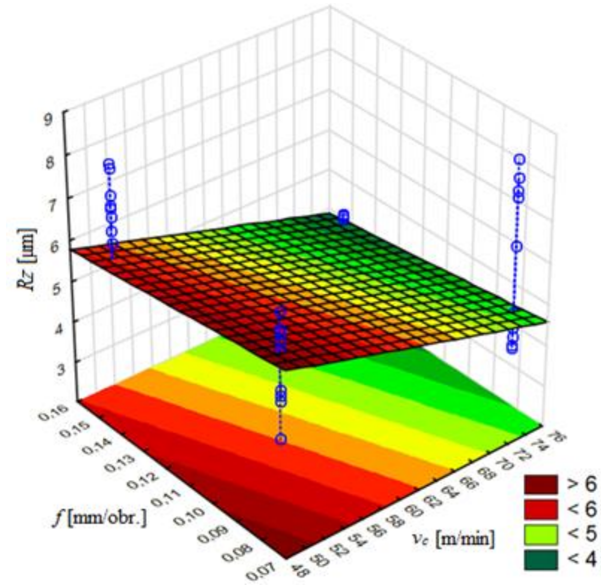

Fig. 14. Rz as a function of cutting speed v_c and feed rate f after turning with SAND CNMG 120408-MF 1115 cutting insert

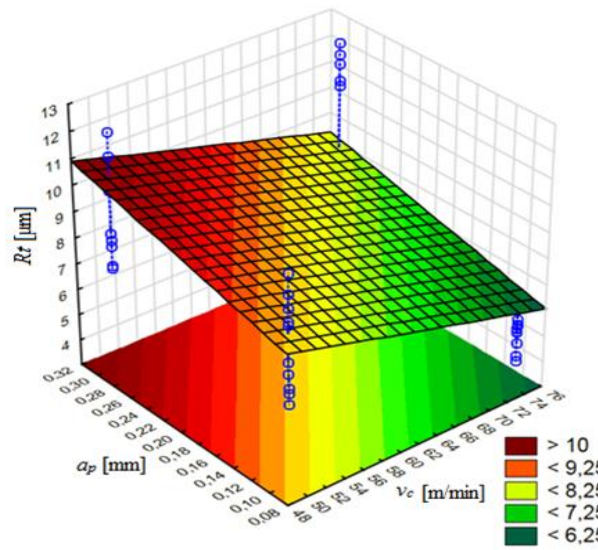

Fig. 15. Rt as a function of cutting speed v_c and cutting depth a_p after turning with SAND CNMG 120408-MF 1115 cutting insert

Fig. 16 shows the evolution of *Rt* as a function of cutting depth a_p and feed rate *f* after turning of 316L stainless steel in laser assisted conditions with SAND CNMG 120408-MF cutting insert. It can be evidenced that the values of *Rt* increase with the decrease of the cutting speed v_c and with the decrease of the feed rate *f*. The highest value of *Rt* is obtained with the cutting speed v_c = 48m/min and with the feed rate *f* = 0,07mm/rev. The lowest value of *Ra* is obtained with the cutting speed v_c = 76m/min and with the feed rate *f* = 0,16mm/rev.

Comparison between the graphs in Fig. 5 – 10 (SECO CNMG 120408-MF1 TM4000 cutting insert) and the graphs in Fig. 11 – 16 (SAND CNMG 120408-MF cutting insert) shows that in turning of 316L stainless steel in LAM conditions with the same technological parameters for both types of cutting inserts, there are different correlations between technological parameters and roughness parameters.

In Fig. 5, the values of *Ra* decrease with the increase of the cutting depth a_p. However, in Fig. 11, the values of *Ra* increase with the cutting depth a_p. Therefore, the correlations between the values of *Ra* and the cutting depth a_p are reversed.

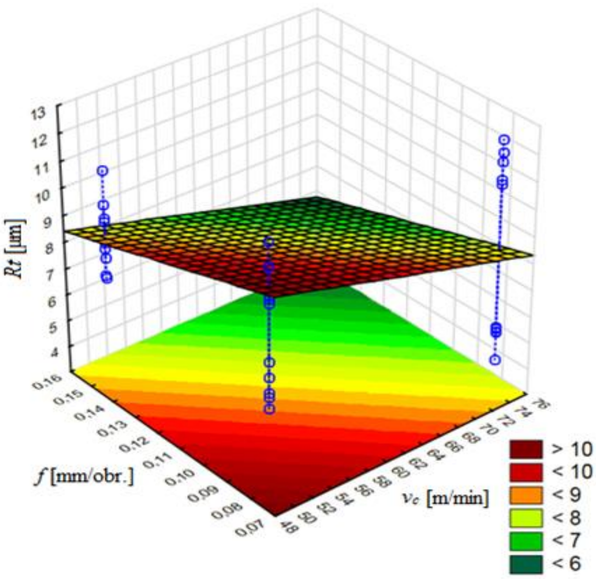

Fig. 16. Rt as a function of cutting speed v_c and feed rate f after turning with SAND CNMG 120408-MF 1115 cutting insert

The graph in Fig. 6 shows that the values of *Ra* increase the feed rate *f*. However, in Fig. 12, the values of *Ra* increase with the decrease of the feed rate *f*. The correlations are reversed.

In Fig. 7, the values of *Rz* decrease with the increase of the cutting depth a_p, while in Fig. 13, the values of *Rz* increase with the cutting depth a_p. In this case, the correlations between the values of *Rz* and the cutting depth a_p are also reversed.

In the first case, Fig. 8 shows that the values of *Rz* increase with the feed rate *f*. On the contrary, Fig. 14 shows that the values of *Rz* increase with the decrease of the feed rate *f*.

The graph in Fig. 9 shows that the values of *Rt* increase with the decrease of the cutting depth a_p, while the graph in Fig. 15 shows that the values of *Rt* increase with the cutting depth a_p. Therefore, the correlations between the values of *Rt* and the cutting depth a_p are reversed.

In Fig. 10, the values of *Rt* increase with the values of the feed rate *f*. However, in Fig. 16, the values of *Rt* increase with the decrease of the feed rate *f*. The correlations are also reversed.

In general, it can be evidenced that the correlations between the values of *Ra*, *Rz* and *Rt* and the values of the cutting speed v_c are the same for both cutting inserts types. The values of *Ra*, *Rz* and *Rt* increase with the decrease of the values of the cutting speed v_c.

4. CONCLUSIONS

The following conclusions can be drawn from the results of this research:

- Technological parameters (cutting speed v_c, cutting depth a_p and feed rate *f*) and cutting tool's microgeometry have influence on geometrical structure of the 316L steel surface after turning in LAM conditions,
- According to the type of cutting insert, there are different correlations between the technological parameters and the surface geometrical structure.
- The values of *Ra*, *Rz* and *Rt* increase with the decrease of the values of the cutting speed v_c.
- In general, it can be evidenced that the values of *Ra*, *Rz* and *Rt* after turning with SECO CNMG 120408-MF1 TM4000 cutting insert decrease with the increase of the values of the cutting depth a_p.
- It can be stated that the values of *Ra*, *Rz* and *Rt* after turning with SAND CNMG 120408-MF cutting insert increase with the values of the cutting depth a_p.
- It can be evidenced that the values of *Ra*, *Rz* and *Rt* after turning with SECO CNMG 120408-MF1 TM4000 cutting insert increase with the values of the feed rate *f*.
- In general, it can be stated that the values of *Ra*, *Rz* and *Rt* after turning with SAND CNMG 120408-MF cutting insert decrease with the increase of the values of the feed rate *f*.
- The decrease of *Ra*, *Rz* and *Rt* parameters with the increase of the feed rate's parameter after turning with SAND CNMG 120408-MF insert is probably caused by the value of cutting edge radius.
- The cutting edge radius, according to Brammers relations, has an influence on the minimum cutting thickness h_{min}.
- Different correlations between the technological parameters and the roughness parameters after turning with different types of cutting inserts are probably caused by differences in structures of chip breakers.
- On the basis of the results of the microscopic measurements of cutting tools, it can be stated that SAND CNMG 120408-MF cutting insert wore more than SECO CNMG 120408-MF1 TM4000 cutting insert.

REFERENCES

[1] **ASM International**, *AK Steel 316L*, ASM International, Ohio 2003.

[2] **Blicharski M.**, *Inżynieria materiałowa. Wydanie czwarte zmienione, Wydawnictwa Naukowo – Techniczne*, Warszawa 2003, 2012 324 – 326.

[3] **Çelik G. A., Polat Ş., Atapek Ş. H., Haidemenopoulos G. N.**, *Microstructural and Mechanical Characterization of Solidified Austenitic Stainless Steels, Archives of Foundary Engineering*, Vol. 17 (3), (2017).

[4] **Dobrzański L. A. (red.)**, *Zasady doboru materiałów inżynierskich z kartami charakterystyk. Wydanie II zmienione i uzupełnione*, Wydawnictwo Politechniki Śląskiej, Gliwice 2001.

[5] **Grądzka-Dahlke M.**, *Analiza procesów zachodzących podczas ściskania porowatej stali 316L do zastosowań biomedycznych*, Eksploatacja i niezawodność, Nr 4/2010.

[6] **Jankowiak M., Przestacki D., Nowak I.**, *Effect of CO2 laser beam applied during machining of SiC particle reinforced aluminium matrix composites*, 5th International PhD Conference on Mechanical Engineering – PhD2007, September 6-8, 2007, Pilsen – Czech Republic.

[7] **Kawalec M., Jankowiak M., Nowakowski Z., Twardowski P., Rybicki M.**, *Hard machining of steel and technical ceramics*, 1st Jubilee Scientific Conference "Manufacturing Engineering in Time of Information Society", Gdańsk, 1st – 2nd June 2006, Department of Manufacturing Engineering and Automation, Gdansk University of Technology.

[8] **Köhnen P., Haase C., Bültmann J., Ziegler S., Schleifenbaum J. H., Bleck W.**, *Mechanical properties and deformation behavior of additively manufactured lattice structures of stainless steel*, Materials and Design 145 (2018) 205 – 217.

[9] **Kotan H.**, *Microstructural evolution of 316L stainless steels with yttrium addition after mechanical milling and heat treatment*, Materials Science & Engineering A 647 (2015) 136 – 143.

[10] **Merchant M. E.**, *Basic mechanics of the metal cutting process*, Journal of Applied Mechanics Transactions of the American Society of Mechanical Engineers (1944) 66:168.

[11] **Szablewski P., Weiss E., Chwalczuk T.**, *Rozwój obróbki materiałów trudnoskrawalnych*, Mechanik, Nr 8–9/2016.